

Manuscript Number: JALCOM-D-15-03882R1

Title: Preparation of Cu(In,Ga)Se₂ photovoltaic absorbers by an aqueous metal selenite co-precipitation route

Article Type: Full Length Article

Keywords: CIGS, selenites, co-precipitation synthesis, amorphous powder, reduction process

Corresponding Author: Mr. Rafael Martí, Ph.D. student

Corresponding Author's Institution: Department of Inorganic and Organic Chemistry, University Jaume I, Av. Sos Baynat, 12071, Castellón de la Plana, Spain

First Author: Rafael Martí, Ph.D. student

Order of Authors: Rafael Martí, Ph.D. student; Leonardo Oliveira; Teodora Stoyanova Lyubenova; Teodor Todorov; Elisabeth Chassaing; Daniel Lincot; Juan Carda

Abstract: In this paper, we report a novel and simple solution-based approach for the fabrication of chalcopyrite Cu(In,Ga)Se₂ thin film solar cells. A novel aqueous co-precipitation method based on metal selenites, M₂(SeO₃)_x (M= Cu, In, Ga) precursors, was investigated. The resulting powder, dispersed in a binder to form an ink, was coated on a substrate by doctor blade technique. A soft annealing treatment enabled the reduction into the corresponding metal selenides leading after rapid thermal processing (RTP) to crystalline chalcopyrite absorber. The obtained layer provides good compositional control and adequate morphology for solar cell applications. Doctor blade printing in atmospheric environment offers an opportunity for direct application of the absorber material at large-scale. The water-based synthesis is a sustainable and simple procedure, and together with doctor blade printing, provides a potential cost-effective advantage over conventional fabrication processes (vacuum-based deposition techniques). The short circuit current (J_{sc}), open circuit voltage (V_{oc}), fill factor (FF), and total area power conversion efficiency (Eff.) of the device are 26 mA/cm², 450 mV, 62%, and 7.2 %, respectively. The effective band gap of 1.12 eV confirmed the Ga-incorporation in the CIGS crystal lattice.

1 Preparation of Cu(In,Ga)Se₂ photovoltaic absorbers by an aqueous metal selenite co- 2 precipitation route

3 R. Martí^{1,*}, L. Oliveira², T. Stoyanova Lyubenova¹, T. Todorov³, E. Chassaing⁴, D. Lincot⁴, J. B.
4 Carda¹

5 ¹ Department of Inorganic and Organic Chemistry, University Jaume I, Av. Sos Baynat, 12071, Castellón
6 de la Plana, Spain

7 ² Department of aerospace science and technology, Institute of Aeronautics and Space - Materials
8 Division, Praça Mal. Eduardo Gomes, 50, 12228-904, São José dos Campos, Brazil

9 ³ IBM T. J. Watson Research Center PO Box 218 Yorktown Heights, NY 10598, USA.

10 ⁴ Institute of Research and Development of Photovoltaic Energy (IRDEP) -UMR 7174-EDF-CNRS-Chimie
11 ParisTech, 6 quai Watier 78401 Chatou Cedex, France.

12

13 * Corresponding Author: Tel: +34 964728234

14 E-mail address: vallsr@uji.es (R. Martí)

15

16 Abstract

17 In this paper, we report a novel and simple solution-based approach for the fabrication
18 of chalcopyrite Cu(In,Ga)Se₂ thin film solar cells. An aqueous co-precipitation method based on
19 metal selenites, M₂(SeO₃)_x (M= Cu, In, Ga) precursors was investigated. The resulting powder,
20 dispersed in a binder to form an ink, was coated on a substrate by doctor blade technique. A
21 soft annealing treatment allowed the reduction of metal selenites into selenides. Further rapid
22 thermal processing (RTP) achieved crystalline chalcopyrite absorber. The obtained layer
23 provides good compositional control and adequate morphology for solar cell applications. The
24 water-based synthesis is a sustainable and simple procedure, and together with doctor blade
25 printing, provides a potential cost- effective advantage over conventional fabrication processes
26 (vacuum-based deposition techniques). The short circuit current (J_{sc}), open circuit voltage (V_{oc}),
27 fill factor (FF), and total area power conversion efficiency (Eff.) of the device are 26 mA/cm²,
28 450 mV, 62%, and 7.2 %, respectively. The effective band gap of 1.12 eV confirmed Ga-
29 incorporation in the CIGS crystal lattice.

30 **Keywords:** CIGS, selenites, co-precipitation synthesis, amorphous powder, reduction process

31

32 1. Introduction

33 Chalcogenide-based solar cells are considered one of the most promising technologies
34 on the market. It has been already attained a record efficiency conversion rate of 21.7% in
35 Cu(In_{0.7}Ga_{0.3})Se₂ (CIGS) thin film cells [1]. These devices also exhibit an excellent long-term
36 stability and durability [2]. In addition, CIGS devices are versatile for deposition on different
37 substrates like glass [1], steel [3], flexible polymeric modules [4] and have been already
38 produced on large scale [5]. High vacuum-based processes like co-evaporation or magnetic
39 sputtering usually deposit CIGS high efficiency devices [6-8]. However, compositional

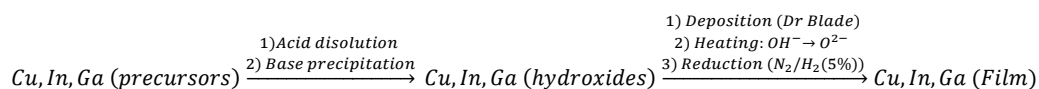
40 heterogeneities issues over large areas are posing challenges for commercial manufacturing
41 [9]. In addition, these methods typically use expensive raw materials and accomplish relatively
42 low materials-utilization efficiency of 70-80% that limits the potential for cost reductions [10].
43 Materials utilization efficiency close to 100% are achievable by non-vacuum processes that
44 deposited the material precisely on the substrate surface [11]. Non-vacuum techniques do not
45 reach the same high efficiencies as the vacuum processes, but they provide lower costs, better
46 large area homogeneity and this would make them highly competitive for future applications
47 [12]. Many non-vacuum routes for chalcogenide-based absorber deposition had already been
48 tested: electrodeposition [13], spin-coating solutions [14, 15] and suspensions of metals [16],
49 oxides [17] and chalcogenides [18].

50 Above all, the solution-based processes are potentially less energy consuming than the
51 vacuum-based approaches that require significantly energy to evaporate or sputter materials
52 from a source onto a heated substrate. Many solution-based methods can deposit precursor
53 layers at room temperature and apply a short treatment technique such as rapid thermal
54 processing (RTP) to form CIGS. This fact will reduce drastically the energy necessities for
55 preparing the solar cells. Solution-based direct printing of inorganic materials offers the
56 possibility of depositing high quality thin films at low temperature under atmospheric
57 conditions for the fabrication of high-performance and ultra-low-cost electronics. Commonly,
58 metal salts (e.g. chlorides and nitrates) are used as direct precursors for CIGS preparation as
59 they have good solubility in water and alcohol. However, these salts are mainly applied in
60 spray-derived processes (e.g. spray pyrolysis) due to their low viscosity solutions formation.
61 The record efficiency of this process is 10.5% [19]. By mixing salts with binders, the viscosity of
62 the solutions may be increased and then sprayed can be employed. In this concept, several
63 solution methods have already been reported. CIGS films made by spin coating using hydrazine
64 as reducing agent have achieved a high efficiency of 12.2% [20]. However, the toxic and
65 explosive nature of hydrazine might limit the large-scale industrial implementation of this
66 exciting approach. Latest, 12% of power conversion efficiency has been obtained on sulfide
67 nanocrystal inks deposited by drop-casting [21]. This is a significant improvement in the non-
68 vacuum technology. But, the hot-injection CIGS synthesis is non-water based. The procedure
69 uses organic solvent (i.e. triethanolamine) and expensive raw materials as metal
70 acetylacetonates.

71 Up to now, there are no reports for using selenites as precursors for CIGS preparation
72 by means of solution-based approaches. Copper, indium and gallium selenites (i.e.
73 $\text{CuSeO}_3 \cdot 2\text{H}_2\text{O}$ [22], $\text{Ga}_2(\text{SeO}_3)_3 \cdot 6\text{H}_2\text{O}$ and $\text{In}_2(\text{SeO}_3)_3 \cdot 6\text{H}_2\text{O}$ [23]) with well-defined crystal
74 structures exist. These compounds associate elements with selenium containing molecules,
75 without direct oxide bonds with the metal atoms. This could be a key advantage for preparing
76 selenides under easier conditions. Thus, chalcogenites could be converted into chalcogenides
77 in presence of amine compounds [24] and during heating in reducing atmosphere [25]. In
78 addition, aqueous and simple way of precursor preparation is essential for future cheap and
79 large-scale manufacturing.

80 Doctor blade deposition technique seems to be the best way for industrial fabrication
81 due to its simplicity and availability at many industrial units. ISET technology developed a doctor
82 blade metallic oxides deposition route [26, 27]. This process is based on a metallic hydroxides

83 precipitation followed by thermal treatment that transforms hydroxide into oxide. Further, the
84 oxides are reduced and selenized according to the reaction (1):



85 $\xrightarrow{\text{Selenization (H}_5\text{Se)}} \text{Cu, In, Ga (selenides)} (1)$

86

87 Good results with efficiencies above 13% were obtained using this route. However, the process
88 is relatively slow. Critical points are metallic oxides attainment from metallic hydroxides
89 (usually requires several hours of heating treatment) and metallic oxides reduction to
90 elemental metals (near of one hour of treatment) [27]. Selenites as precursors simplify the
91 process thanks to their easy reduction to selenides thereby decreasing production time of
92 absorber layer.

93 In the present work, which follows a preliminary study by T. Todorov [28], we propose
94 an easy solution-based chemistry route as aqueous co-precipitation of metal selenites for
95 precursor preparation. Further, deposition of ink using doctor blade techniques was applied in
96 order to develop CIGS absorbing layer. The water- based synthesis is a safety, sustainable and
97 simple procedure. The precursor powders and the developed layers have been detailed
98 characterized in terms of structural, microstructural, and electrical properties.

99

100 2. Materials and methods

101 • Sample Preparation

102 All chemicals were used as received without further purification. Cu(NO₃)₂·3H₂O (99%,
103 Fluka), In(NO₃)₃·xH₂O (99.99%, Aldrich), Ga(NO₃)₃·xH₂O (99.9%, Aldrich), SeO₂ (99.8%,
104 Aldrich) and ammonia solution NH₄OH (25%, Panreac). Precursor solution was obtained by
105 dissolving copper (2.52 mmol), indium (1.96 mmol) and gallium (0.84 mmol) nitrates in 125 mL
106 of distilled water with a final metal ratio of [Cu]/([In]+[Ga])= 0.9 and [Ga]/([In]+[Ga])=0.3 [7].
107 Separately, 10 mmol SeO₂ was dissolved in distilled water, resulting in a colorless transparent
108 solution. Ammonia was added in one single batch to obtain the desired precipitate. The
109 powder was washed with water and ethanol and then centrifuged. No additional purification
110 was needed.

111 To make the ink, triethanolamine (C₆H₁₅NO₃ puriss., Riedel-de Haën, as surfactant and
112 reducer) and ethanol (C₂H₅OH Abs., Scharlau, abbreviated as EtOH,) were used. The obtained
113 paste was deposited by a simplified doctor blade method (knife coating) on Mo-coated (~500
114 nm-thick layer) glass substrates. The substrate was heated at 400 °C for 1 minute on a hot
115 plate in order to obtain partial decomposition of organic components and selenite reduction.
116 Then a crystallization treatment is carried out in a rapid thermal processing (RTP) furnace
117 (Jetfirst 100, JIPELEC) formed by a sealed annealing zone water cooled and a heating element
118 which consists of 12 infrared halogen lamps with individual power of 1200 W. At 550 °C during

119 5 minutes under 5% H₂/N₂ stationary atmosphere with a heat rate of 500 °C/min. Elemental
120 selenium powder (Se, 99.5%, Merck) was introduced separately into the furnace as selenium
121 source.

122 Solar cells assemblies were completed by adding of chemically-bath deposited CdS and
123 sputtered i-ZnO/ZnO:Al coatings.

124 • Characterization

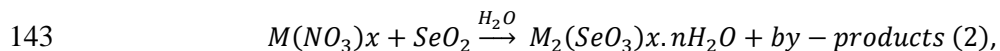
125 The crystal structure of the materials was characterized by X-ray powder diffraction (XRD)
126 with a SIEMENS D5000D diffractometer with a copper anticathode. The data were collected by
127 step-scanning from 20 to 70° 2θ with a step size of 0.05° 2θ and 1s counting time per step. The
128 X-ray photoelectron spectra (XPS) of the samples were recorded with a SPECS apparatus
129 equipped with a Phoibos 100 analyzer and a 5MCD detector. The morphology of powders and
130 films were determined by Scanning Electron Microscopy (SEM), using a Leica Leo 440i
131 microscope, and Transmission Electron Microscopy (TEM) applying a JEOL 2100 microscope.
132 Both instruments were equipped with a spectrometer for Energy dispersive X-ray energy
133 spectroscopy (EDS). Current-voltage (I-V) characteristics of the solar cells were carried out
134 using a solar simulator in standard illumination conditions: AM 1.5 and 100 mW/cm², with a
135 cell size of 0.1 cm².

136 3. Results and discussion

137 The CIGS absorber layers were obtained after a three stage process:

- 138 1) Metal-selenites formation by obtaining precipitated mixed powder.
- 139 2) Doctor-blade deposition and pre-heating of precipitated selenites.
- 140 3) Thermal crystallization process (RTP).

141 The metal selenite powder was obtained by reaction of the metal nitrate salts with
142 selenium oxide solutions according to reaction (2):

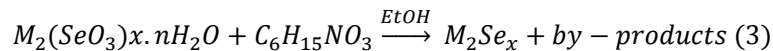


144 Where M= Cu, In and Ga. The nature of the by-products is still unclear.

145 It is noticeable that the selenite precipitate associates the metal and the chalcogene
146 element, because metal-selenium (selenite) bond allows a rapid reduction to metal-selenide.
147 The TEM micrograph of the precipitated powder (Fig. 1a) shows nanocrystal agglomerates with
148 average size of ~0.5 μm. The agglomerates are formed by small particles with dimensions close
149 to 35 nm. Several regions of the sample were analyzed by EDS. The results describe average
150 elemental composition of the powder (more than 30 areas had been analyzed) closed to the
151 initial stoichiometry (1:0.78:0.33 atomic ratio of Cu/In/Ga). The values of Cu (25.6%), In
152 (21.3%), Ga (7.6%) and Se (45.6%) correspond to the 1:0.83:0.3 (Cu/In/Ga) atomic metal ratios.
153 It can be concluded that the developed method reach a homogeneous compound. As shown
154 by the X-Ray diffraction pattern (Fig. 2, curve 1), the powder displays an amorphous structure.

155 **Fig. 3** displays the XPS spectrum of the as-prepared precipitate. The binding energy of
 156 XPS peaks corresponding to levels In3d (In3d_{3/2} at 444.4 eV, In3d_{1/2} at 452.2 eV) and Ga2p_{3/2} (at
 157 1117.7 eV) indicates that the oxidation states of the group 3 metallic cations are In³⁺ and Ga³⁺
 158 [29], the same oxidation state as the initial salts. Also, the peak observed at 58.64 eV is related
 159 to Se3d, indicating that selenium oxidation state is 4+ (i.e. selenite species SeO₃²⁻) [29]. The
 160 peaks at 932 eV and 952 eV represent the levels Cu2p_{3/2} and Cu2p_{1/2}, respectively. However,
 161 these reflections do not establish unambiguously the oxidation state of Cu. The Cu¹⁺ and Cu²⁺
 162 have a very similar response [29]. The XPS spectrum of Cu²⁺ should show a very wide additional
 163 peak centered at 942.5 eV with similar intensity to the Cu2p_{1/2} [30]. However, this peak is not
 164 detected even at the zoomed in-set view (**Fig. 3** in-set) that suggests only the presence of Cu¹⁺
 165 species. This is a surprising result since no deliberate reducing agent is added in the solution. A
 166 possible explanation would be the effect of the addition of ammonia for the precipitation
 167 according to some papers that show the reducing properties of NH₃ [31, 32]. The presence of
 168 Cu¹⁺ avoids extra reduction procedures.

169 Then the powder is dispersed into the binder and deposited as a layer on the Mo
 170 covered glass substrate. Afterward, the layer is submitted to a soft annealing treatment on a
 171 hot plate at 400°C for 1 min in air. The XRD pattern reveals three main peaks that may be
 172 associated with chalcopyrite-type material (**Fig. 2** curve 2). The appearance of these peaks is
 173 associated with a reduction reaction provoked by the amines nature [24]. The results show
 174 accordance to the reaction (3):



175 Since triethanolamine have been added for the ink preparation, the selenites, for
 176 which selenium is tetravalent, have been reduced into selenides where selenium is at
 177 oxidation state -2, leading to CIGS compound, although not complete Ga-insertion was
 178 achieved. **Fig. 1b** shows the SEM cross section of the pre-treated at 400°C film. It displays that
 179 the CIGS layer is compact and adherent with a uniform thickness close to 3 μm.

180 A crystallization heat treatment is then carried out in N₂/H₂ (5%) atmosphere together
 181 with a selenium source at 550°C in a RTP furnace. **Fig. 2** curve 3 shows that the CIGS
 182 chalcopyrite phase is obtained as a main crystalline phase. The diffraction peaks labeled with
 183 *hkl* could be assigned to the CuIn_{0.7}Ga_{0.3}Se₂ (JCPDS card No. 35-1102). Additional peaks at 40.5°
 184 and 73.6° (2θ) can be attributed to molybdenum (Mo) from the layer behind. Reflections
 185 centered at 31.8° (2θ) and 55.9° (2θ) (labeled as star *) could be associated to a formation of
 186 molybdenum selenide at the interface CIGS/Mo (MoSe₂ JCPDS card No. 40-0908). The chemical
 187 reaction between selenium and Mo layer is very common in CIGS devices, due to interdiffusion
 188 processes [33]. Nevertheless, the presence of MoSe₂ does not harm the electrical properties of
 189 the cell. The zoomed area in **Fig. 2** displays a comparison of reflection (112) in the curves 2
 190 and 3. It can be observed that on the curve 2 appears a small shoulder (+) next to the principal
 191 peak. The reflections (220) and (312) in curve 2 also demonstrate additional peaks. The
 192 presence of these shoulders and peaks at higher angles are related to gallium partial insertion
 193 (presence of gallium-rich phase). The heating applied (curve 3) decreases the shoulder and
 194 displace the peak (112) toward higher angles. This is a demonstration of unit cell volume

195 reduction that is consistent with $r\text{Ga}^{3+} < r\text{In}^{3+}$. This is a confirmation of the gallium
196 incorporation in the crystal lattice [34].

197 **Fig. 1c** shows the cross section of a finished cell. The assembly of the solar cell was
198 completed by adding CdS buffer and i-ZnO/ZnO:Al window layers. It shows that the thickness
199 of the CIGS layer is decreased to 1.2 μm , due to decomposition of organic components coming
200 from the binder. Although carbon presence decreased after annealing treatment, it was still
201 possible to observe it by EDX analysis of CIGS layer located mostly near of interface MoSe₂-
202 CIGS. The presence of a carbon layer is usually reported when organic compounds are used in
203 order to deposit absorber layers [35, 36]. Formation of MoSe₂ layer with similar to Mo
204 columnar morphology located at the interface CIGS/Mo is also observed. This is in agreement
205 with the DRX results previously discussed (**Fig. 2**). Unclear separation between the CdS buffer
206 (~ 40 nm) and the window films i-ZnO/ZnO:Al is observed. Only EDS analysis confirms the
207 presence of these elements in the cell (data not shown).

208 The current-voltage (I-V) characteristics for the optimal CIGS solar cell measured under
209 standard AM 1.5 illumination are shown in **Fig. 4**. The as-fabricated device shows an efficiency
210 of 7.2% and good cell parameters ($V_{\text{OC}} = 450$ mV, $J_{\text{SC}} = 26$ mA/cm² and FF = 62%). The current
211 density values of the record efficiency sample were determined by quantum efficiency
212 measurements (**Fig. 5**) and the J_{SC} value obtained in J-V curve were close to each other (24.5
213 and 26 mA/cm² respectively). The quantum efficiency showed a good collection of
214 photogenerated electron-hole pairs, yielding values close to 75% in the short wavelength
215 range. Towards longer wavelengths, the quantum efficiency decreases, which indicates low
216 collection length (space charge width plus diffusion length of electrons) values. This result
217 (quantum efficiency showed high carrier collection at short wavelengths) indicates that
218 collection length can be further improved. The effective band gap determined from the
219 spectral response was 1.12 eV indicating gallium incorporation in the chalcopyrite lattice. To
220 compare, the effective values of record performance devices exhibit band gap value of 1.14 eV
221 for composition $\text{Ga}/(\text{In}+\text{Ga}) = 0.3$ [7].

222 4. Conclusions

223 A novel soft chemistry route is developed based on the formation of metal selenite-
224 based precursor powders for CIGS preparation by aqueous co-precipitation. Doctor blade
225 technique was used as an easy and cheap way of paste deposition. A key point of the process
226 is the internal reduction of the selenites into selenides through a mild annealing technique.
227 The formation of crystalline CIGS layer with good morphological properties confirms the
228 effectiveness of the developed method of preparation. The coatings are dense, well adhered
229 and uniform. The electrical response of the CIGS cell yielded an efficiency of 7.2%. The
230 effective band gap of 1.12 eV confirmed the Ga-incorporation in the CIGS crystal lattice.
231 Further studies of ink composition and thermal crystallization treatment could remove or
232 decrease carbon on the absorber layer and improve CIGS crystallinity thus getting better
233 electric parameters.

234

235

236 Acknowledgments

237 This work was supported by the Spanish Ministry of Science and Competiveness under
238 INNFACTO Program (IPT-2011-0913-920000). The authors would like to thanks to Manuel
239 Ocaña Jurado (ICMS-CISC) for his help in the XPS measurements. L. Oliveira would like to thank
240 the support of the National Council for Scientific and Technological Development (CNPq) –
241 Brazil.

242

243 References

- 244 [1] P. Jackson, D. Hariskos, R. Wuerz, O. Kiowski, A. Bauer, T.M. Friedlmeier, M. Powalla,
245 Properties of Cu(In,Ga)Se₂ solar cells with new record efficiencies up to 21.7%, physica status
246 solidi (RRL) – Rapid Research Letters, 9 (2015) 28-31.
- 247 [2] M.A. Green, K. Emery, Y. Hishikawa, W. Warta, Solar cell efficiency tables (Version 31),
248 Progress in Photovoltaics: Research and Applications, 16 (2008) 61-67.
- 249 [3] R. Wuerz, A. Eicke, F. Kessler, S. Paetel, S. Efimenko, C. Schlegel, CIGS thin-film solar cells
250 and modules on enamelled steel substrates, Solar Energy Materials and Solar Cells, 100 (2012)
251 132-137.
- 252 [4] A. Chirilă, P. Bloesch, S. Seyrling, A. Uhl, S. Buecheler, F. Pianezzi, C. Fella, J. Perrenoud, L.
253 Kranz, R. Verma, D. Guettler, S. Nishiwaki, Y.E. Romanyuk, G. Bilger, D. Brénaud, A.N. Tiwari,
254 Cu(In,Ga)Se₂ solar cell grown on flexible polymer substrate with efficiency exceeding 17%,
255 Progress in Photovoltaics: Research and Applications, 19 (2011) 560-564.
- 256 [5] Z. Wei, P.R. Bobbili, S. Senthilarasu, T. Shimell, H.M. Upadhyaya, Design and optimisation of
257 process parameters in an in-line CIGS evaporation pilot system, Surface and Coatings
258 Technology, 241 (2014) 159-167.
- 259 [6] J. Liu, D. Zhuang, H. Luan, M. Cao, M. Xie, X. Li, Preparation of Cu(In,Ga)Se₂ thin film by
260 sputtering from Cu(In,Ga)Se₂ quaternary target, Progress in Natural Science: Materials
261 International, 23 (2013) 133-138.
- 262 [7] I. Repins, M.A. Contreras, B. Egaas, C. DeHart, J. Scharf, C.L. Perkins, B. To, R. Noufi, 19.9%-
263 efficient ZnO/CdS/CuInGaSe₂ solar cell with 81.2% fill factor, Progress in Photovoltaics:
264 Research and Applications, 16 (2008) 235-239.
- 265 [8] P. Jackson, D. Hariskos, E. Lotter, S. Paetel, R. Wuerz, R. Menner, W. Wischmann, M.
266 Powalla, New world record efficiency for Cu(In,Ga)Se₂ thin-film solar cells beyond 20%,
267 Progress in Photovoltaics: Research and Applications, 19 (2011) 894-897.
- 268 [9] L. El Chaar, L.A. Lamont, N. El Zein, Review of photovoltaic technologies, Renewable and
269 Sustainable Energy Reviews, 15 (2011) 2165-2175.
- 270 [10] M. Leihern, Challenges for vacuum system manufacterrers in the PV industry. Workshop
271 Proceeding of the Third International Workshop. Thin Films in the Photovotaic Industry 2007,
272 Ispra, Italy.
- 273 [11] C.J. Hibberd, E. Chassaing, W. Liu, D.B. Mitzi, D. Lincot, A.N. Tiwari, Non-vacuum methods
274 for formation of Cu(In, Ga)(Se, S)₂ thin film photovoltaic absorbers, Progress in Photovoltaics:
275 Research and Applications, 18 (2010) 434-452.
- 276 [12] T. Todorov, D.B. Mitzi, Direct Liquid Coating of Chalcopyrite Light-Absorbing Layers for
277 Photovoltaic Devices, European Journal of Inorganic Chemistry, 2010 (2010) 17-28.
- 278 [13] S. Ji, P. Yang, J. Zhang, Y. Lian, J. Zhang, M. An, Electrodeposition of CuIn_xGa_{1-x}Se₂ from a 1-
279 butyl-3-methylimidazolium trifluoromethanesulfonate ionic liquid, Materials Letters, 133
280 (2014) 14-16.
- 281 [14] L. Oliveira, T. Todorov, E. Chassaing, D. Lincot, J. Carda, P. Escribano, CIGSS films prepared
282 by sol-gel route, Thin Solid Films, 517 (2009) 2272-2276.

283 [15] Y. Liu, D. Kong, J. Li, C. Zhao, C. Chen, J. Brugger, Preparation of Cu(In,Ga)Se₂ Thin Film by
284 Solvothermal and Spin-coating Process, *Energy Procedia*, 16 (2012) 217-222.

285 [16] B.M. Başol, Low cost techniques for the preparation of Cu(In,Ga)(Se,S)₂ absorber layers,
286 *Thin Solid Films*, 361–362 (2000) 514-519.

287 [17] Z.-L. Liu, F.-S. Chen, C.-H. Lu, Synthesis and characterization of copper gallium diselenide
288 powders prepared from the sol–gel derived precursors, *Ceramics International*, 39 (2013)
289 8641-8647.

290 [18] C.-H. Chung, B. Bob, B. Lei, S.-H. Li, W.W. Hou, Y. Yang, Hydrazine solution-processed
291 CuIn(Se,S)₂ thin film solar cells: Secondary phases and grain structure, *Solar Energy Materials*
292 *and Solar Cells*, 113 (2013) 148-152.

293 [19] M.A. Hossain, Z. Tianliang, L.K. Keat, L. Xianglin, R.R. Prabhakar, S.K. Batabyal, S.G.
294 Mhaisalkar, L.H. Wong, Synthesis of Cu(In,Ga)(S,Se)₂ thin films using an aqueous spray-
295 pyrolysis approach, and their solar cell efficiency of 10.5%, *Journal of Materials Chemistry A*, 3
296 (2015) 4147-4154.

297 [20] W. Liu, D.B. Mitzi, M. Yuan, A.J. Kellock, S.J. Chey, O. Gunawan, 12% Efficiency CuIn(Se,S)₂
298 Photovoltaic Device Prepared Using a Hydrazine Solution Process†, *Chemistry of Materials*, 22
299 (2009) 1010-1014.

300 [21] Q. Guo, G.M. Ford, R. Agrawal, H.W. Hillhouse, Ink formulation and low-temperature
301 incorporation of sodium to yield 12% efficient Cu(In,Ga)(S,Se)₂ solar cells from sulfide
302 nanocrystal inks, *Progress in Photovoltaics: Research and Applications*, 21 (2013) 64-71.

303 [22] A. Larrañaga, J.L. Mesa, L. Lezama, M.I. Arriortua, T. Rojo, Mild Hydrothermal Synthesis of
304 Cu(SeO₃).2H₂O: Structural Characterization, Thermal, Spectroscopic and Magnetic Studies,
305 *Spectrochimica Acta Part A: Molecular and Biomolecular Spectroscopy*, 72 (2009) 356-360.

306 [23] L.T. Vlaev, M.M. Nikolova, G.G. Gospodinov, Non-isothermal kinetics of dehydration of
307 some selenite hexahydrates, *Journal of Solid State Chemistry*, 177 (2004) 2663-2669.

308 [24] W.C. Benzing, Process for preparing metal selenides, in, Google Patents, 1960.

309 [25] L.T. Vlaev, G.G. Gospodinov, Study on the kinetics of the isothermal decomposition of
310 selenites from IIIB group of the periodic system, *Thermochimica Acta*, 370 (2001) 15-19.

311 [26] V.K. Kapur, A. Bansal, P. Le, O.I. Asensio, Non-vacuum processing of CuIn_{1-x}Ga_xSe₂ solar
312 cells on rigid and flexible substrates using nanoparticle precursor inks, *Thin Solid Films*, 431–
313 432 (2003) 53-57.

314 [27] V.K. Kapur, B.M. Basol, C.R. Leidholm, R.A. Roe, Oxide-based method of making compound
315 semiconductor films and making related electronic devices, in, Google Patents, 2000.

316 [28] T.K. Todorov, Preparation and study of thin films for photovoltaic applications, in:
317 *Inorganic and Organic Chemistry Department, Universitat Jaume I, Castellón de la Plana*
318 (Spain), 2008, pp. 223.

319 [29] W.H.R. C. D. Wagner, L. E. Davis, J. F. Moulder, G. E. Muilenberg, *Handbook of X-Ray*
320 *Photoelectron Spectroscopy*, Minnesota, 1973.

321 [30] J.P. Espinós, J. Morales, A. Barranco, A. Caballero, J.P. Holgado, A.R. González-Elipe,
322 Interface Effects for Cu, CuO, and Cu₂O Deposited on SiO₂ and ZrO₂. XPS Determination of the
323 Valence State of Copper in Cu/SiO₂ and Cu/ZrO₂ Catalysts, *The Journal of Physical Chemistry B*,
324 106 (2002) 6921-6929.

325 [31] T. Curtin, F. O' Regan, C. Deconinck, N. Knüttle, B.K. Hodnett, The catalytic oxidation of
326 ammonia: influence of water and sulfur on selectivity to nitrogen over promoted copper
327 oxide/alumina catalysts, *Catalysis Today*, 55 (2000) 189-195.

328 [32] F. Nishida, T. Yamada, N. Suzuki, T. Takeda, T. Yanagihara, K. Adachi, T. Asanabe, K.
329 Ohsato, K. Tsuda, Process for removal of nitrogen oxides from waste gas, in, Google Patents,
330 1978.

331 [33] T. Wada, N. Kohara, S. Nishiwaki, T. Negami, Characterization of the Cu(In,Ga)Se₂/Mo
332 interface in CIGS solar cells, *Thin Solid Films*, 387 (2001) 118-122.

333 [34] M. Venkatachalam, M.D. Kannan, S. Jayakumar, R. Balasundaraprabhu, N.
334 Muthukumarasamy, Effect of annealing on the structural properties of electron beam
335 deposited CIGS thin films, *Thin Solid Films*, 516 (2008) 6848-6852.
336 [35] V. Haug, A. Quintilla, I. Klugius, E. Ahlswede, Influence of an additional carbon layer at the
337 back contact-absorber interface in Cu(In,Ga)Se₂ thin film solar cells, *Thin Solid Films*, 519
338 (2011) 7464-7467.
339 [36] M. Kaelin, D. Rudmann, F. Kurdesau, H. Zogg, T. Meyer, A.N. Tiwari, Low-cost CIGS solar
340 cells by paste coating and selenization, *Thin Solid Films*, 480–481 (2005) 486-490.

341

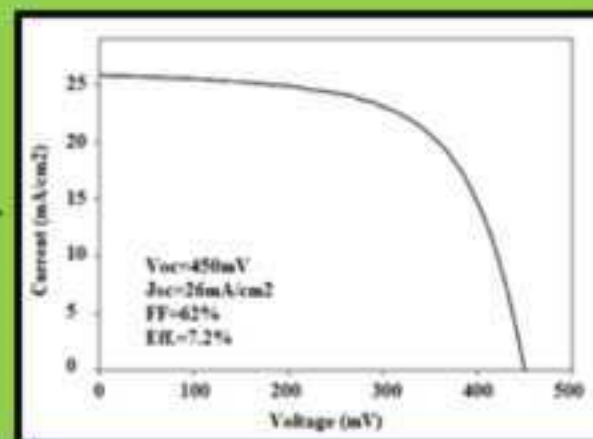
342



Aqueous co-precipitation
of Metal-selenites



Hot-plate reduction
treatment (1 min, 400°C)



Electrical measurements

Highlights:

- CIGS photovoltaic solar cell was prepared by aqueous co-precipitation route.
- CIGS layer was obtained depositing paste by doctor blade technique.
- Efficiency of 7.2% and Ga-incorporation in the CIGS crystal lattice was achieved.

Figure 1
[Click here to download high resolution image](#)

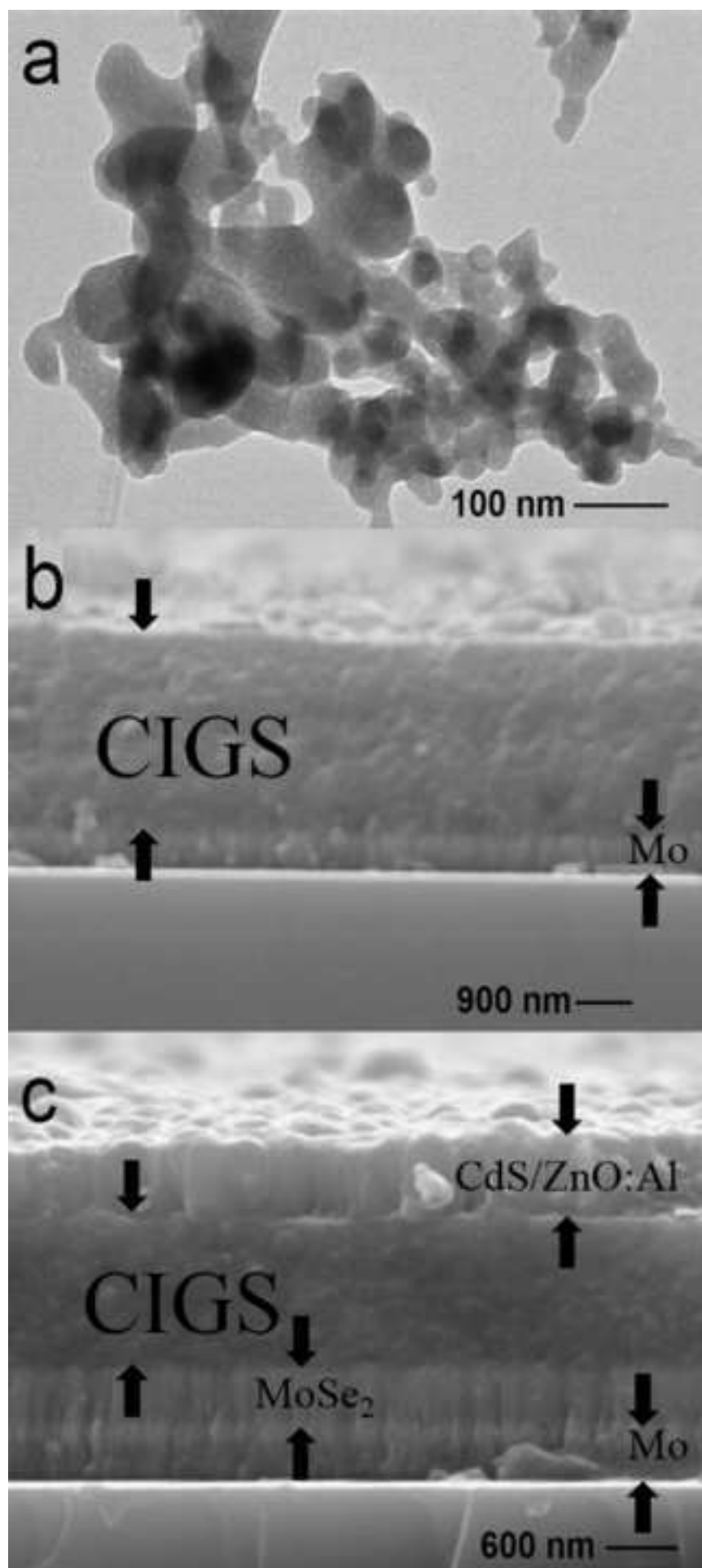


Figure 2
[Click here to download high resolution image](#)

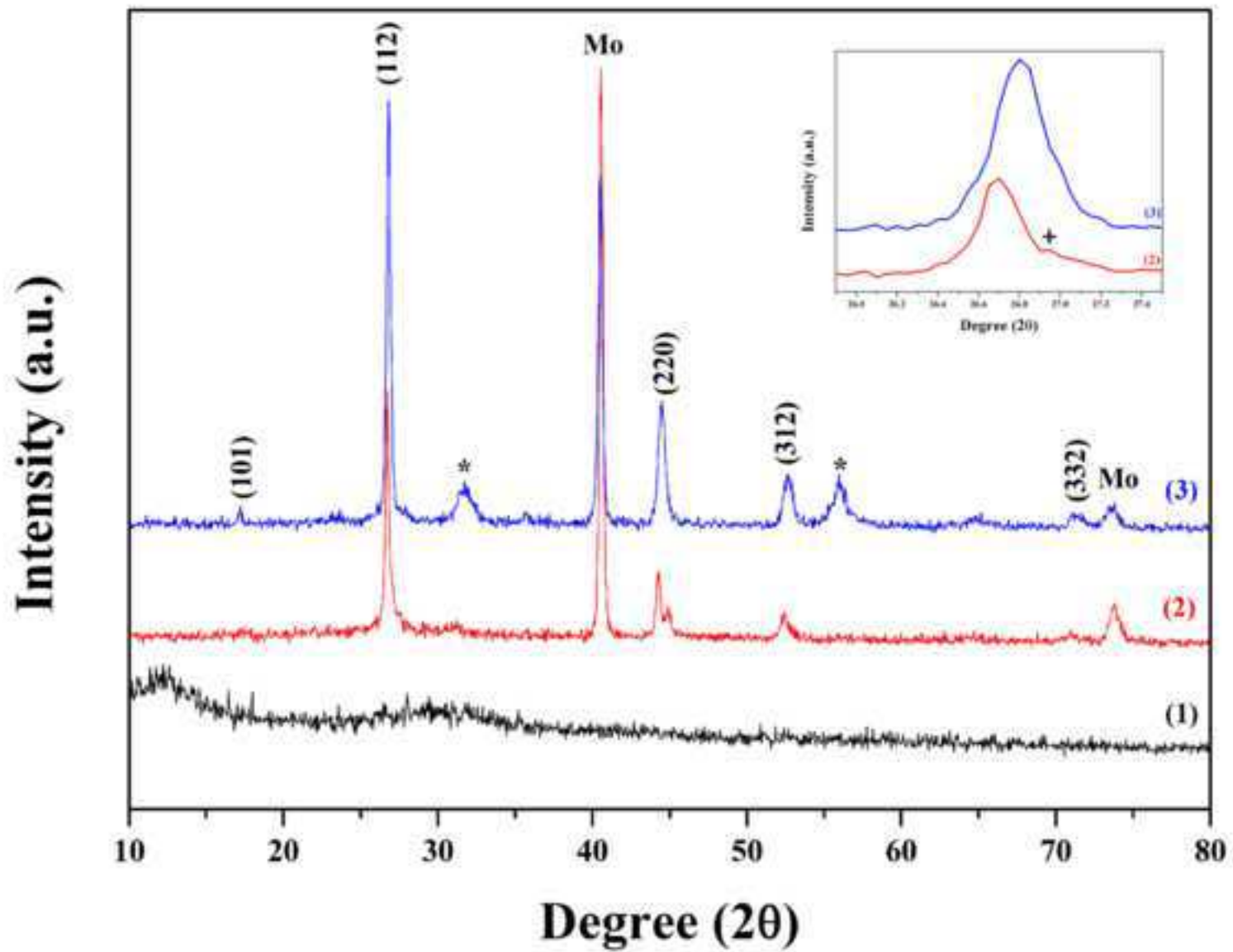


Figure 3
[Click here to download high resolution image](#)

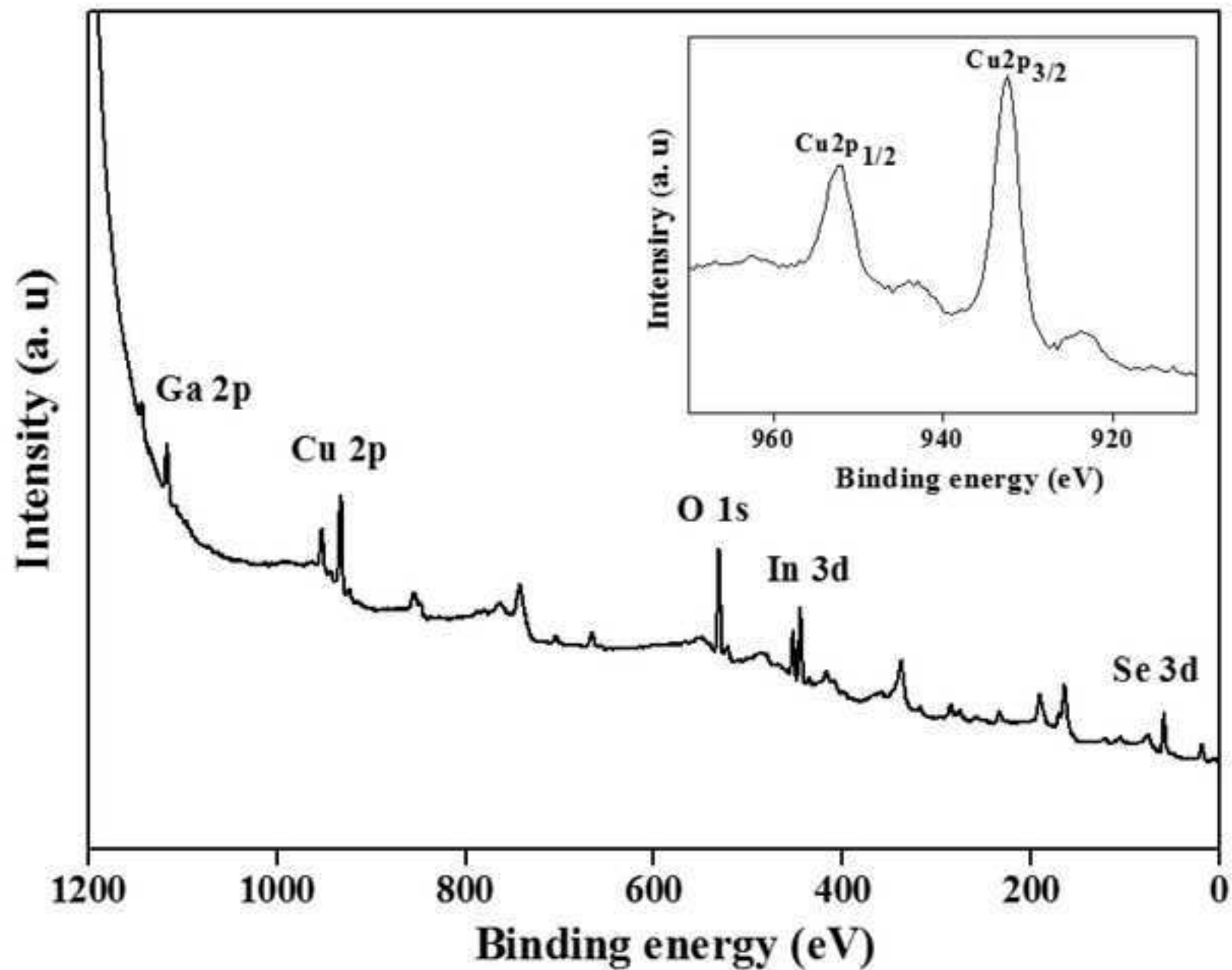


Figure 4
[Click here to download high resolution image](#)

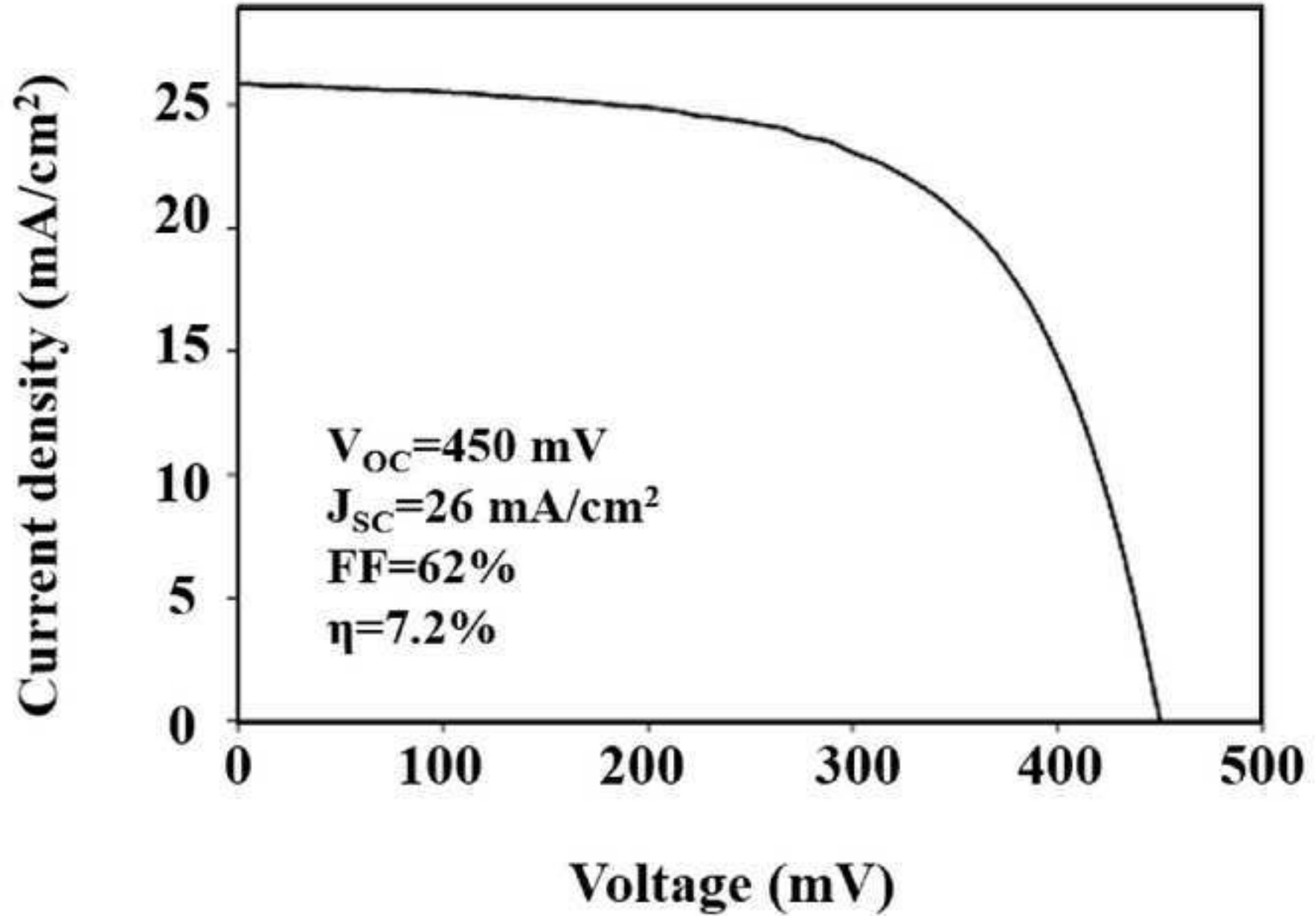


Figure 5
[Click here to download high resolution image](#)

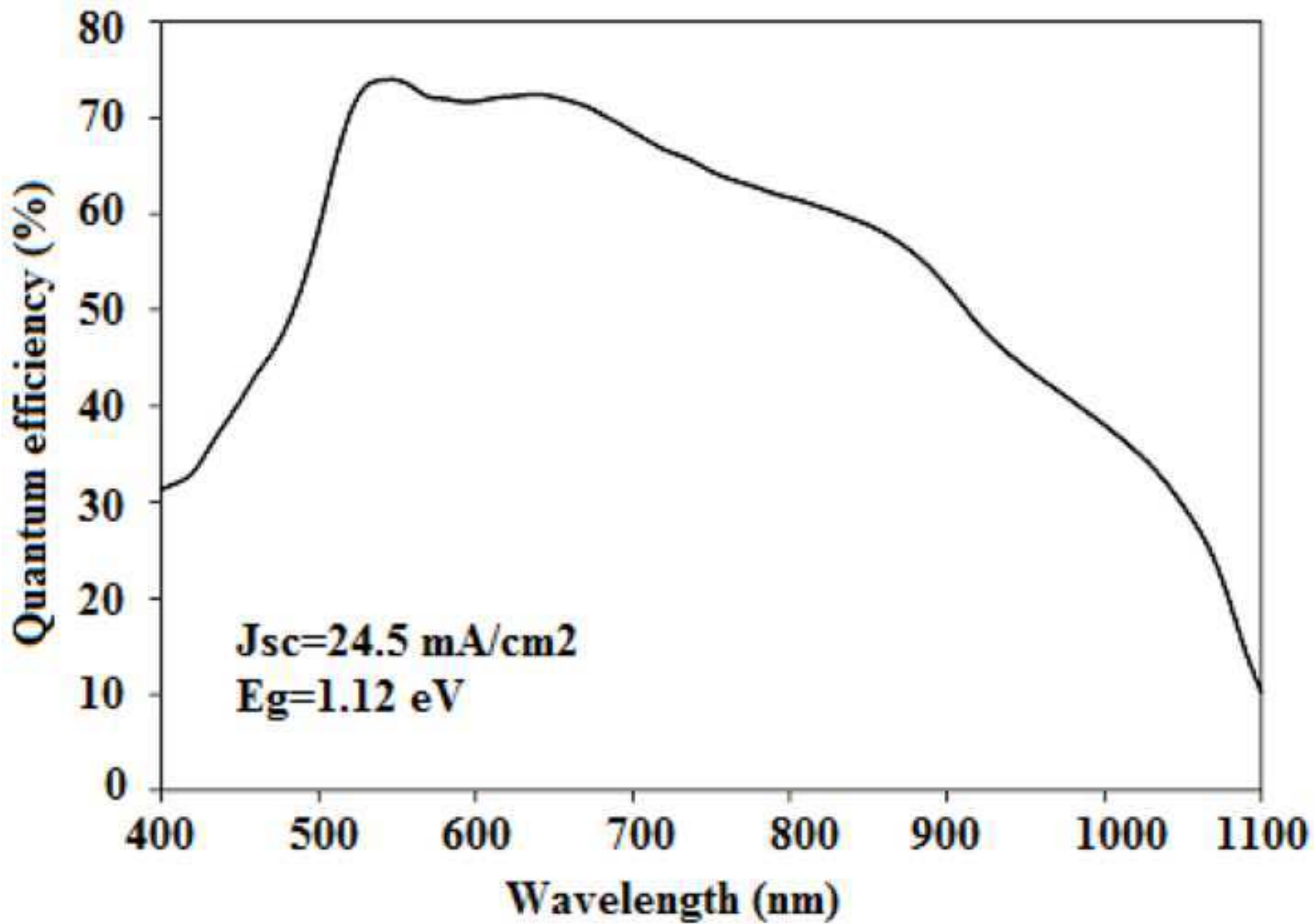


FIGURE CAPTIONS

Figure 1: Micrographs of: (a) TEM image of precursor powder, (b) SEM cross section of a pre-treated at 400°C film and (c) SEM view of a final solar cell assembly.

Figure 2. XRD patterns of Cu-In-Ga-Se sample: 1-as-prepared precursor precipitate (lower), 2-pre-heated at 400°C film (intermediate) and 3-thermal treated at 550°C coating (upper). Reflections indexed by hkl correspond to $\text{Cu}(\text{In}_{0.7}\text{Ga}_{0.3})\text{Se}_2$. Peaks labeled as stars (*) are associated to MoSe_2 .

Figure 3. XPS spectrum of Cu-In-Ga-Se as-prepared powder. Inset view: zoomed section of Cu2p peaks

Figure 4 - I-V curve of the best CIGS solar cell under illumination

Figure 5. External Quantum efficiency of the best CIGS solar cell.